Palaeogeography, Palaeoclimatology, Palaeoecology 534 (2019) 109313

Contents lists available at ScienceDirect

Palaeogeography, Palaeoclimatology, Palaeoecology

journal homepage: www.elsevier.com/locate/palaeo

Aragonite pteropod abundance and preservation records from the Maldives, equatorial Indian Ocean: Inferences on past oceanic carbonate saturation and dissolution events

E. Sreevidya[a], A.V. Sijinkumar[a,*], B. Nagender Nath[b]

[a] Department of Geology, Central University of Kerala, Kasaragod, India
[b] CSIR-National Institute of Oceanography, Dona Paula, Goa, India

ARTICLE INFO

Keywords:
Calcification
Limacina dissolution index
Mid-Brunhes Dissolution Interval
Paleoceanography
Ventilation

ABSTRACT

During the International Ocean Discovery Program (IODP) Expedition 359, a long continuous carbonate-rich sequence was recovered from the Inner Sea of Maldives. We investigated pteropod proxies (absolute abundance of pteropods species, total pteropods, epipelagic to mesopelagic ratio, fragmentation ratio, *Limacina* Dissolution Index (LDX), mean shell size variations of *L. inflata*) from Sites U1467 (water depth: 487 m) and U1468 (water depth: 521 m) to understand both surface and sub-surface paleoceanographic changes in the equatorial Indian Ocean and to improve our understanding of the factors responsible for pteropod preservation on longer time-scales. A total of 15 species of pteropods were identified, and their downcore variations were documented from the core top to 707.49 mbsf in U1467 and from 447.4 to 846.92 mbsf in U1468. At the Site U1467, pteropod shells show high abundances/preservation up to a depth of 45 mbsf (~1.2 Ma), which is consistent with the presence of aragonite content in sediments (with the top 50 m bearing high aragonite content). Beyond 45 mbsf, only fragmented pteropod shells were seen down to 50 mbsf (corresponding to 1.5 Ma) followed by a total absence of pteropod shells and fragments from 50 mbsf (~1.5 Ma) to the end of the core at 846.92 mbsf (~24 Ma). A decrease in the SO_4^{2-}concentration and alkalinity in the interstitial fluid geochemistry is seen at these depths. The presence of dolomite content below 50 mbsf also indicates the alteration of aragonite into dolomite. Analyses of the carbonate preservation proxies reveal that the pteropods exhibit considerable fluctuation in abundance/preservation during the last 1.2 Myr. A good to moderate preservation (LDX: 2 to 3) is seen which correlates well with the fragmentation ratio but with an inverse relation with calcification rate. The proxies for in-life pteropod shell dissolution (average size of *L. inflata* and LDX) indicate that glacial periods (MIS 16, 14, 6, 4 and 2) have shown no signs of dissolution pointing better calcification under aragonite-saturated water column which is in good correlation with reduced atmospheric CO_2 concentration. Epipelagic/mesopelagic ratio indicates that the water column exhibited enhanced ventilation and mixing during glacial to interglacial periods, but intervals of intense stratification, a sign of poor ventilation or weakened circulation, was prevalent beyond MIS 14. The longest interval of poorest preservation was marked during MIS 11 and 13, which corresponds to the 'Mid-Brunhes Dissolution Interval (MBDI).' On a longer time scale, the abundances/preservation of pteropods in the Maldives seems to be controlled by changes in the seawater chemistry associated with monsoon productivity, water column ventilation, and atmospheric CO_2 concentration.

1. Introduction

Euthecosomatous pteropods are a ubiquitous and abundant group of holoplanktonic, pelagic mollusks belonging to class Gastropoda and secreting aragonitic tests which contribute significant amounts of calcareous materials to marine sediments, particularly in tropical and subtropical latitudes (e.g., Herman, 1968; Orr et al., 2005). The abundance of pteropods within different water-masses depend upon physico-chemical properties, and by the adaptive potential of different individual species, hence they can record the past ocean conditions in postmortem shells. Owing to the larger size and mass than that of foraminifera shells, pteropod tests have a higher settling velocity that promotes deposition close to their habitat (Kalberer et al., 1993). The distribution and preservation of aragonite shells in the seafloor

* Corresponding author.
E-mail address: sijingeo@gmail.com (A.V. Sijinkumar).

https://doi.org/10.1016/j.palaeo.2019.109313
Received 15 February 2019; Received in revised form 24 July 2019; Accepted 1 August 2019
Available online 05 August 2019
0031-0182/

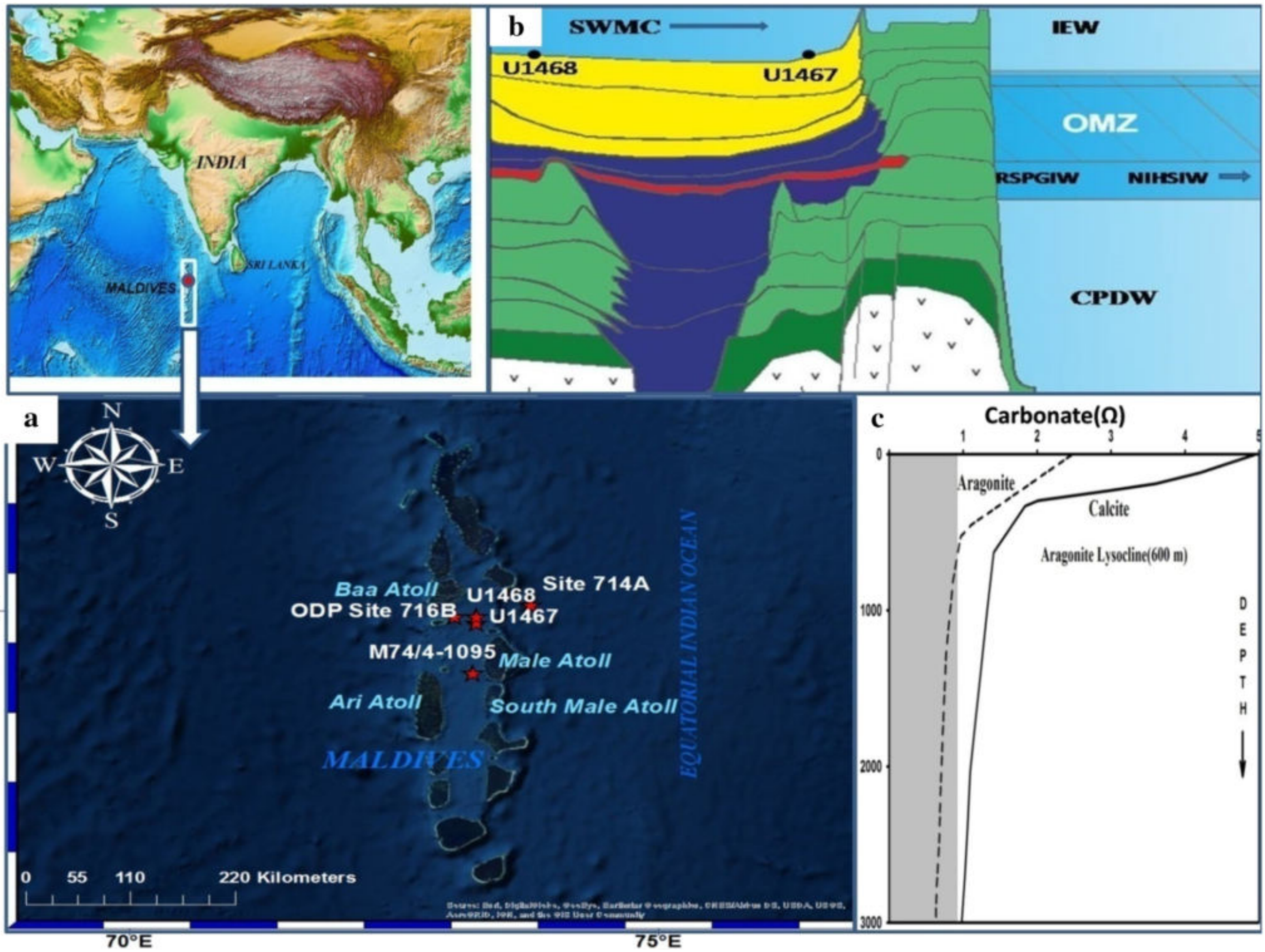

Fig. 1. Study area with core locations, carbonate saturation profile, and water-masses. (a) Enlarged core location sites with respect to key islands. Location of the Indian Ocean (1) IODP Expedition 359 Site U1467 (water depth: 428 m) (2) IODP Expedition 359 Site U1468 (water depth: 531 m) in the Maldives, along with the previous locations where studies have been conducted, such as (3) *R/V Meteor* piston core M74/4–1095 on the western slope of Malé Atoll (water depth: 328 m) (modified from Paul et al., 2011), (4) ODP Leg 115 Site 716 near the middle of Kaashidhoo channel (water depth: 540 m) (modified from Droxler et al., 1990; Cullen and Droxler, 1990; Sarkar and Gupta, 2009), and (5) (a) ODP Leg 115 Site 714 Hole A, 30 km southeast of Fadiffolu Atoll (water depth: 2195 m), (b) modern water-masses around the Maldives with the relative position of IODP Expedition 359 Site U1467 and U14698. Water-masses include Indian Equatorial Water (IEW), Red Sea-Persian Gulf Intermediate Water (RSPGIW) and Circumpolar Deep Water (CDW). Currents include Summer South West Monsoon Current (SWMC) and North Indian High Salinity Intermediate Water (NIHSIW). Oxygen Minimum Zone (OMZ) for the Arabian Sea is applied to this area, producing an ALy at 600 m. (Information from Emery, 2001; Sabine et al., 2002; modified from Sarkar and Gupta, 2009; Wall-Palmer et al., 2013),and (c) Aragonite profile of the Indian Ocean (Böning and Bard, 2009; Reid et al., 2009). (For interpretation of the references to colour in this figure legend, the reader is referred to the web version of this article.)

sediments provide important information about the carbonate chemistry of the oceans and the paleoceanographic signatures (e.g., Gerhardt et al., 2000; Gerhardt and Henrich, 2001). The aragonite records were effectively used to interpret the paleoclimate, ocean circulation and history of ocean water chemistry (Gardner, 1975; Crowley, 1983, [CSL STYLE ERROR: reference with no printed form.]; Droxler et al., 1983; Howard and Prell, 1994; Böning and Bard, 2009; Wall-Palmer et al., 2013).

Recent studies are more concerned about the effect of ocean acidification upon calcifying organisms like pteropods and highlight that the thecosomatous pteropods are at high risk (Orr et al., 2005; Fabry et al., 2008; Comeau et al., 2012; Bednaršek et al., 2012a, 2012b). Increased dissolved CO_2 concentration leads to decreased water pH and low carbonate concentration, causes reduced calcification rates, and enhances dissolution in the shells of living pteropods (e.g., Wall-Palmer et al., 2013). It has been found that although pteropods can calcify in under-saturated water with respect to aragonite, the rate of calcification is reduced and enhanced dissolution corrodes the surface layer of their shells (Comeau et al., 2012). This results in the production of smaller, weaker shells with damaged outer aragonite layer (Bednaršek et al., 2012b; Wall-Palmer et al., 2013). Several criteria have been commonly used as indicators of the intensity of carbonate dissolution in deep-sea sediments. Among them, *Limacina* Dissolution Index (LDX), which is the widely used proxy to assess the scale of pteropod shell dissolution, is designed to determine the depth of aragonite lysocline (Aly). *Limacina inflata* is an abundant species in the tropical ocean; their shells have a helical aragonite microstructure (Bé and Gilmer, 1977) which makes them more susceptible to dissolution than other species of *Limacina*, thus are extremely useful for comparing LDX record. Recent studies using calcification (from *L. inflata* average shell-size data) and LDX (as a proxy of in-life shell dissolution) have shown that the low atmospheric CO_2 concentration and the resulting high surface-water carbonate saturation coincide with the presence of large shells and low in-life dissolution during glacial periods in a 450 kyr record (Wall-Palmer et al., 2013).

There are not many long-term continuous records of pteropods since

Miocene from the Indian Ocean even though they are known to occur since the Cretaceous. The preservation of the pteropods during the last 55 kyr in the Andaman Sea has shown an inverse relationship with atmospheric CO_2 concentration (Sijinkumar et al., 2015). Hence, pteropod microfossils can be effectively used as a proxy for paleoclimate and, more specifically, ocean acidification driven by natural fluctuation in the CO_2 concentration on longer time scales. A recent study from the Indian Ocean has revealed the anthropogenic effects on aragonite preservation (Sabine et al., 2002). The aragonite saturation depth has shoaled significantly by 25–155 m in the Indian Ocean due to the absorption of anthropogenic CO_2 in the subsurface water-masses and also due to increasing inorganic-matter decomposition rates (Sabine et al., 2002; Sarma et al., 2002). The present-day, aragonite saturation level in the Indian Ocean is significantly shallower than that of the pre-industrial time.

The deepest aragonite saturation is found in the southwestern Indian Ocean, and the saturation horizon then shoals toward the northeast to a minimum of 200–400 m in the Bay of Bengal (Sabine et al., 2002; Sarma et al., 2002). The production and composition of biogenic carbonate in the equatorial Indian Ocean are related to environmental conditions of surface-waters that are under the direct influence of the unique monsoon climatic and oceanographic settings of the northern Indian Ocean (Cullen and Droxler, 1990). Thus, it is crucial to understand the past records of ocean acidification driven by natural causes on the longer timescale for future modeling and predictions. The present study attempts to assess the preservation record of aragonitic pteropod shells from the Maldives, the Indian Ocean, in cores from IODP Expedition 359, which provides a complete Neogene record of the platform and platform margin sediments. A comparison with the pelagic records over the same time period would allow us to assess the extent to which platform carbonates record changes in the global carbon cycle (see Swart et al., 2019). The advantage with the drill sites of IODP Expedition 359 is that the water depths of drill sites are above the Aragonite lysocline and thus the changes in pteropod preservation are not influenced by shifts in lysocline.

2. Oceanographic settings

The Maldives archipelago is an isolated tropical carbonate-platform located in the Equatorial Indian Ocean and thus ideal for studying the pelagic sedimentation. A North-South oriented double row of atolls (about 1200 smaller atolls) encloses the Inner Sea of the Maldives (Fig. 1). The Inner Sea is characterized by periplatform ooze deposition (Droxler et al., 1990; Malone et al., 1990), locally accumulated into sediment-drift bodies (Betzler et al., 2009, 2013a, 2013b; Lüdmann et al., 2013). Passages separate the atolls formed during the partial demise of larger carbonate banks along with the drift deposition during the middle Miocene at 13 Ma (Aubert and Droxler, 1996; Betzler et al., 2009, 2013a, 2013b, 2016; Lüdmann et al., 2013). The climate and oceanographic setting of the Maldives are dictated by the seasonally reversing Indian monsoon system (Tomczak and Godfrey, 2003). The strong south-westerly winds prevail from mid May to November, accompanied by eastward currents and torrential rainfall (south-west monsoon, wet season; Schott et al., 2009) and primary productivity reaches its maximum in September, i.e. at the end of the southwest monsoon, but is moderate compared to high-productivity areas of the Arabian Sea (Schulte et al., 1999). However, the upwelled water is overlain by a thin low-salinity layer (510 m thick), which results from local precipitation (Schulte et al., 1999). The effect of upwelling, therefore, is small though the thermocline is shallow. A reversed pattern of wind and ocean currents is developed from January to March, with meager precipitation rates (northeast monsoon, dry season). A deepening of the mixed layer is observed during the northeast monsoon, but without an increase in primary productivity owing to the inflow of low salinity surface waters from the Bay of Bengal (Schulte et al., 1999). The mean annual temperatures lie between 25.7 °C and 30.5 °C, with the highest temperatures observed in April and the lowest in December. Mean annual precipitation is 1924.7 mm for the central Maldives, with precipitation maxima occurring from May to December. The Maldives are thus among the few carbonate platforms which have developed in a regime of strong annual changes in wind and current patterns (Paul et al., 2011). The IODP Expedition 359 results have proved that the currents were established abruptly, in response to the onset of the Indian Monsoon around 12.9 Ma (Betzler et al., 2016, 2018). Water-masses include the Indian Equatorial Water (IEW), Red Sea-Persian Gulf Intermediate Water (RSPGIW) and the Circumpolar Deep Water (CDW). Currents include the summer South West Monsoon Current (SWMC) and the North Indian High Salinity Intermediate Water (NIHSIW) (Emery, 2001; Sabine et al., 2002).

3. Material and methods

The easternmost Site U1467 (4°51.0274′N, 073°17.0223′E, water depth: 487 m) in the Inner Sea of Maldives was drilled during International Ocean Discovery Program (IODP) Expedition 359. The site is located 24.8 km east of the eastern end of the northern transect, and 29.4 km east of the eastern end of the southern transect and represents drift deposits. Site U1468 is located in the Kardiva channel in the Inner Sea (4°55.9823′N, 073°4.2834′E, water depth: 521 m) of Maldives (Fig. 1). The Site U1468 has platform-related sediments overlain by a thick succession of current-controlled deposits that allow for dating the age of the onset of the drifts which is related to the onset of the Indian monsoon (Betzler et al., 2018). Both sites together provide a complete Neogene record of the platform and platform margin sediments (Betzler et al., 2016, 2017, 2018). Pteropods were studied from both of these sites in which three hundred and forty-eight samples were analyzed from Site U1467 (~12.48 Myr old sediment sequence), rich in foraminifera, nannofossils and pteropods ranging from ~1500 kyr to present and 29 samples from Site U1468 ranging from ~25 Myr to 12 Myr (ages from chronological models provided in site reports, Betzler et al., 2017). Samples were soaked in water for 8–12 h and washed with a jet of water over a 63 μm size sieve. The washed samples retained on the sieve were dried in an electric oven at ~42 °C, and the dried sediments were transferred into labeled vials. The dried filtrate was sieved through 150 μm mesh sieve. The samples were split into several aliquots to reduce the total number to a minimum of 300 individuals. Care was taken to avoid mechanical damage of the shells. The sample was then weighed using an analytical balance, and the number of pteropods presented in the paper refers to this original weight. The coarse fraction (> 150 μm) was used for quantitative and qualitative analysis of pteropods assemblages under a stereo zoom binocular microscope. The pteropod species were identified following Van der Spoel (1967), Bé and Gilmer (1977) and Almogi-Labin (1982). All pteropod shells were identified, counted, and computed as an absolute number per gram of dry sediment. Pteropod fragments were also counted, and the fragmentation ratio was calculated using the expression $n_F/(n_F + n_W)$, where n_F is the number of fragments and n_W is the number of whole tests (Klöcker et al., 2006). The various indirect dissolution proxies, pteropod abundances, and dissolution index of *L. inflata* were used to assess the state of aragonite preservation. Following Gerhardt and Henrich (2001), preservation stages (scale 0–5) were assigned to *L. inflata* of size > 150 μm for each sample, and the LDX is calculated using the expression, LDX = Σ (N p*p)/ ΣN p, where N p represents the number of investigated tests per preservation stage, p (0–5). The downcore variations in all the six stages of *L. inflata* and their abundances are also studied and compared with other results. The average shell size of *L. inflata* was also measured as an indicator of shell calcification (following Wall-Palmer et al., 2013). Epipelagic and mesopelagic species ratio was used to delineate the past ventilation changes. Attempts have been made to compare the data with the existing records of Pleistocene pteropod abundances, LDX and average shell size of *L. inflata*, atmospheric CO_2 record, and monsoon productivity proxies. The

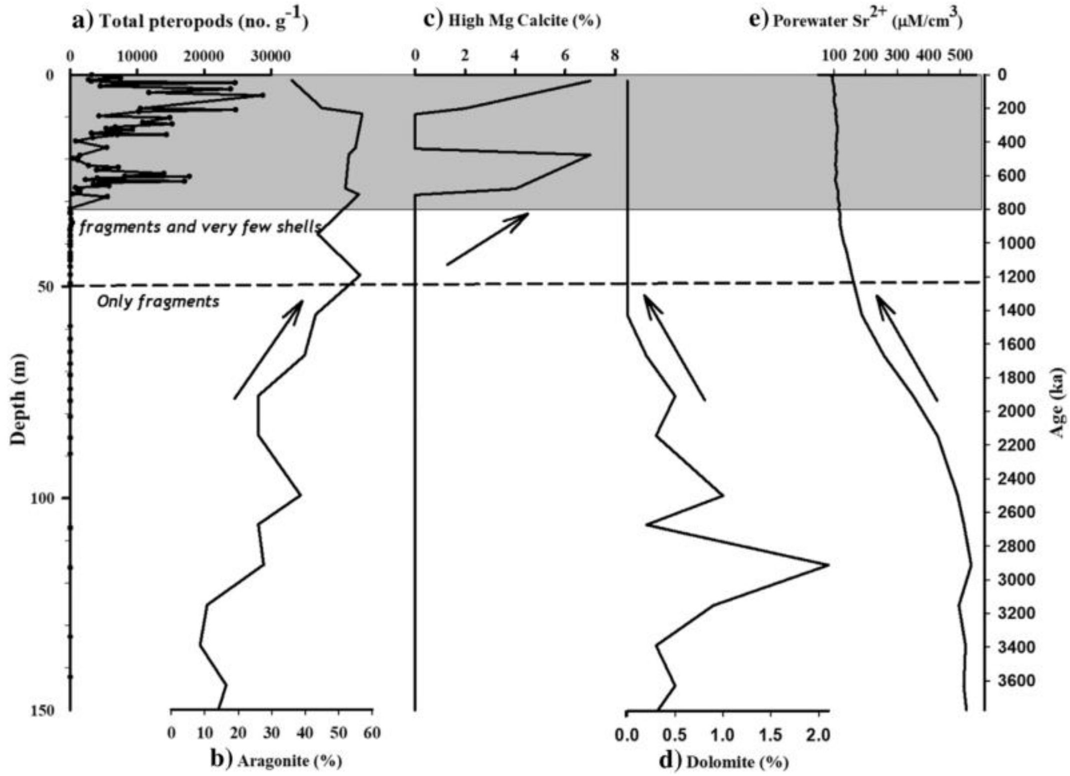

Fig. 2. (a) Downcore variation of total pteropods (no. g^{-1}) plotted against depth and age, (b) aragonite content (%), (c) High-Mg Calcium (%), (d) dolomite content (%) in sediments & (e) Sr^{2+} (μM/cm^3) in pore-water with depth and age. The shaded box indicates the depth range up to which pteropod shells are preserved. The dotted line marks the depth where pteropod shell fragmentation sets out maximum. The arrow marks indicate the variations in pore-water chemistry and dolomite (%) in sediments in relation with remineralization/alteration of aragonite.

core collection, sampling techniques, lithostratigraphy, age models, mineralogy, and geochemical data have been previously published for Sites U1467 and U1468 in IODP Proceedings (Betzler et al., 2016, 2017).

4. Results

4.1. Pteropod species abundances/preservation

Total pteropod data from IODP 359 Site U1467 are presented in Fig. 2 and compared with the aragonite, high-Mg calcite (HMC`), dolomite and pore-water Sr^{2+} content for depicting the relationship between the geochemistry of the sediments and fossilized aragonite shells. The present study has yielded rich assemblages of 15 pteropod species from Site U1467, and their downcore abundance per gram of sediments is presented in Fig. 3. There are no pteropod shells or its fragments present from 447.4 to 846.92 mbsf at Site U1468. The presence of encrusted or lumps of foraminifera shells which are filled with sediments/minerals are present in distinct intervals in the lower part of the core of Site U1467 (below 48 mbsf) (See Betzler et al., 2017). Further downcore, there are no whole pteropod shells, but only fragments are present which slowly grades into recrystallized/remineralized lumps (below 60 mbsf) (Figs. 2 and 3). The mesopelagic *L. inflata* is the dominant species and comprises about 60 to 70% of the total assemblages. Downcore, the species abundance varies considerably, with peaks (> 50%) during glacial stages. During MIS 11 and 13, the abundance/preservation was very low. The epipelagic species *L. trochiformis*, associated with upwelling, ranks second in absolute abundance and shows the highest abundance during MIS 6–7. Mesopelagic upwelling species *L. bulimoides* ranked third among the pteropods in absolute abundance and was rare during MIS 2, 6, and 8 but was more common during MIS 5, 7 and 14. In general, these two species are more abundant during interglacial stages. *Creseis virgule* s.l. includes variants like *C. virgula virgula, C. virgula conica,* and *C. chierchiae* and ranks fourth in abundance. These three species belonging to the epipelagic group live in the mixed layer (Bé and Gilmer, 1977). In general, the absolute abundance of *C. virgule* s.l. was higher during the interglacial stages. *Styliola subula* ranked fifth and were abundant during MIS 5. *Cavolinia gibbosa*, a mesopelagic species, is the next most abundant which were plentiful during interglacial sections. A rare bathypelagic species, *Clio polita* which was documented by Ivanova (1985) in Red Sea sediments, was encountered at certain depths corresponding to MIS 2, 5 and 16. *Clio cuspidata, Diacria quadridentata, C.convexa, C. pyramidata, C. acicula,* and *D. trispinosa* are the least abundant species among the other pteropods which are abundant during interglacial to glacial transition stages. Also, the pteropod abundance falls to less than one hundred shells from MIS 16 to MIS 19 (Fig. 3).

4.2. Mesopelagic vs. epipelagic species

The ratios of mesopelagic to epipelagic species are estimated to understand the past ventilation changes in the water column (Fig. 4). In the present study, it is found that mesopelagic species were abundant over epipelagic, and the ratio is high during some of the interglacial periods. The significant increase in mesopelagic species abundance was demarcated during MIS 3, 4, MIS 6 to MIS 5 transition, MIS 8 to MIS 7 transition, and MIS 14 to MIS 13 transition periods. On the other hand, epipelagic species abundance was high during MIS 2 to 1 transition, MIS 7 to 6 transitions, MIS 10 to 9 transitions and beyond MIS 15. The ratio exhibited high values when epipelagic species were plenty over mesopelagic species.

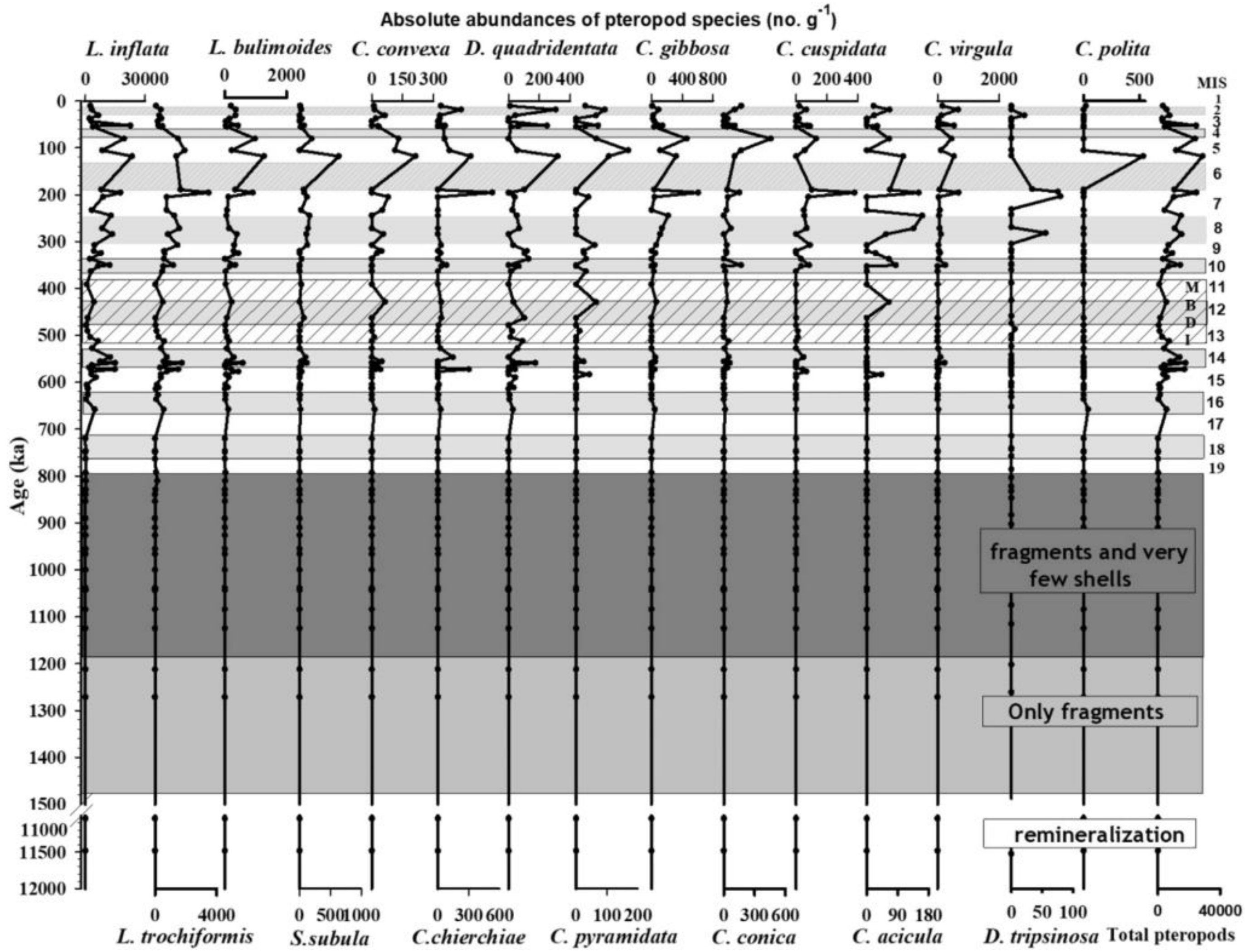

Fig. 3. Downcore variations in the absolute abundance (no. g^{-1}) of all the pteropod species and total pteropods in Core Site U1467 with respect to age and glacial-interglacial stages. Shaded portion marks MBDI.

4.3. Aragonite dissolution and calcification proxies

The state of aragonite shell preservation varies throughout the record (Fig. 5). The six different classes of preservation used by Almogi-Labin et al. (1986) were applied here. The scale extends from 0 (best; pristine, transparent shells) to 5 (worst; opaque-white, totally lusterless and perforated shells). In the present investigation, two intervals of major variation in the mode of preservation were observed. The least altered shells of the *L. inflata* were common during glacial periods, and mostly corroded shells were observed during interglacial periods. In most of the record, the majority of pteropod shells are preserved with their original aragonite shells. Quantitatively, they are more abundant during MIS 2, 6, and 12. The in-life pteropod dissolution was determined using the LDX (Fig. 5) and does not show much variation until 800 kyr since most of the values fall between 2 and 3 preservation stages, which indicate moderate preservation (i.e., opaque white shells lustrous to partly lusterless shell surface). In general, relatively higher values of preservation stage (more corroded) are noted during interglacial stages. The interval of higher dissolution occurred during the Mid-Brunhes Dissolution Interval (MBDI). Further down, LDX values hit the highest points. A considerable amount of pteropod fragments are found in samples at the deeper depths which show higher values during most of the interglacial stages. The number of pteropod fragments increases considerably downcore and is higher during interglacial, MBDI, MIS 18 and 1000 kyr to 790 kyr. Fragmentation ratios correlate with LDX, and are moderate up to 700 kyr, but amplify rapidly with depth. LDX data are compared with that of the ODP Site 716B record (Wall-Palmer et al., 2013) and found that the data is well matching, where glacial (interglacial) periods are marked by lower (higher) dissolution index and vice versa. Good correlation in LDX values between ODP Hole 716B and Site U1467 was seen during MIS 2 and MIS 6 (Fig. 5).

The average shell size of *L. inflata* was measured as an indicator of shell calcification (Wall-Palmer et al., 2013). The shell size was calculated by measuring the diameter perpendicular to the line of aperture on the spiral side using a photomicroscope. Measurements were made for all appropriate shells (> 150 µm) that had been picked from a count of 300 pteropod and foraminifera specimens for each sample and presented as an average. Shell sizes were found to be smaller during interglacial stages, suggesting reduced calcification (Fig. 5). Average shell size can also be used to rule out the post-depositional dissolution of pteropod shells. Preferential dissolution of smaller shells leaves larger, stout preserved shells. Total pteropods records of Site U1467 were compared with the limited published records of pteropod preservation, atmospheric CO_2 record and monsoon productivity proxies for the last 800 kyr, which exhibit good correlation with the pteropod preservation/abundances (Fig. 6). In general, the preservation maximum corresponds to the glacial stages when CO_2 in the atmosphere was minimum. Pteropod based (pteropods fragmentation ratio and LDX)

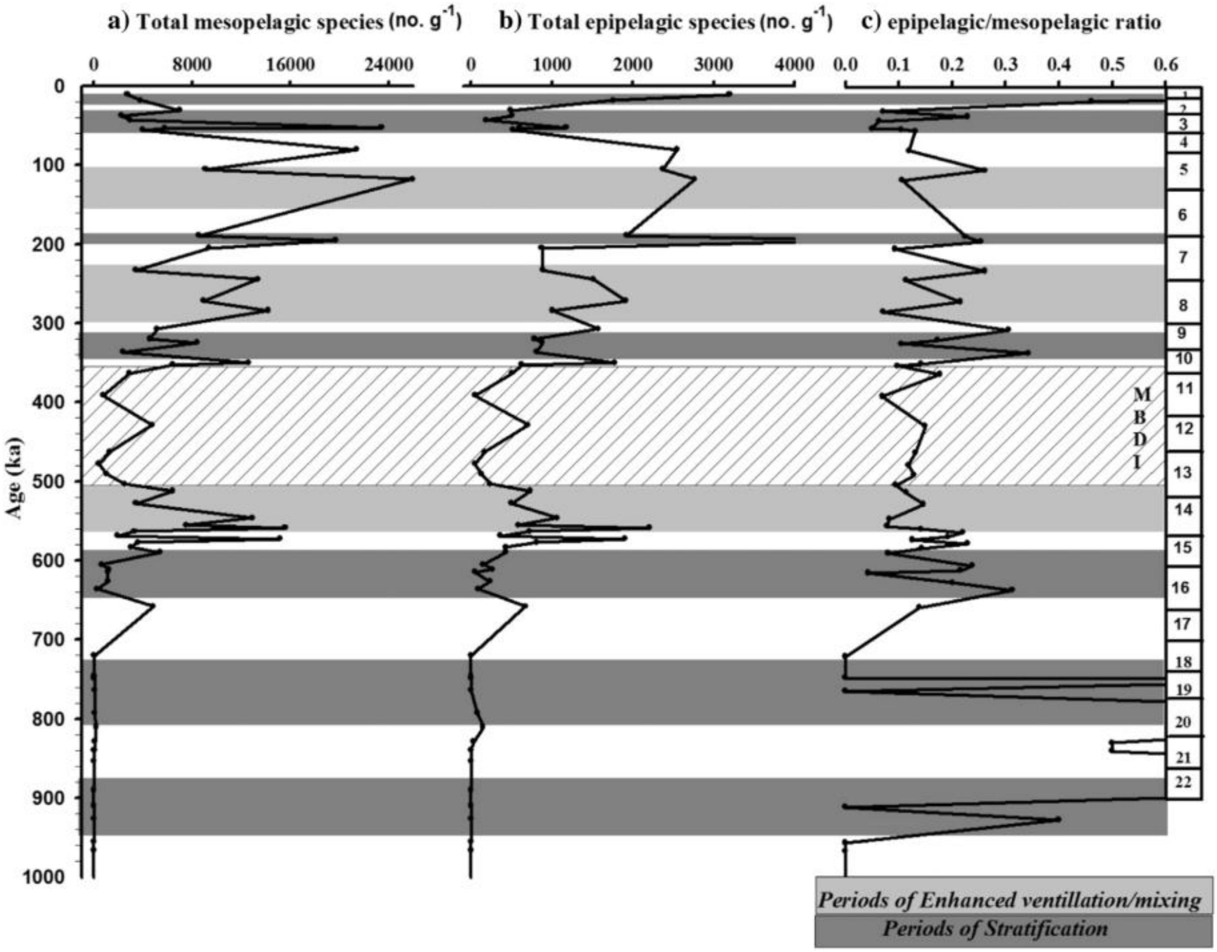

Fig. 4. (a) Total mesopelagic (no. g^{-1}) (b) total epipelagic species (no. g^{-1}) and (c) epipelagic/ mesopelagic ratio for water column changes plotted against age with MIS. Periods of enhanced ventilation and stratifications are marked using variations in the abundance/preservation of pteropods of different depth habitats.

carbonate dissolution data are compared with previously published foraminifera dissolution index (foraminifera fragmentation ratio and foraminifera preservation index), which are given in Fig. 7.

5. Discussion

5.1. Mineralogical changes at the expense of pteropod dissolution

The well-preserved fossil pteropods shells are found only during the last 800 kyr (Site U1467) coinciding with high aragonite content in the sediments (45–55%; Betzler et al., 2017) (Fig. 2). The presence of pteropods shells and fragments coincides with the decrease in aragonite content (Fig. 2). Deeper down, mere fragments followed by the complete absence of pteropods are noticed (Figs. 2 and 3), suggesting the carbonate remineralization at a depth of 60 mbsf (1500 ka) which is also supported by changes in pore-water SO_4^{2-} and alkalinity (Betzler et al., 2017). The depth of reduction in well-preserved pteropod shells with an increase in the presence of their fragments coincides with an increase in the dolomite content at 55 mbsf, suggesting the formation of dolomite at the expense of aragonite dissolution (Fig. 2). In the upper ~50 mbsf, the sediment consists of a small amount of HMC (See Betzler et al., 2017). This precipitation of HMC is often associated with aragonite dissolution. So the decrease in pteropods could be a consequence of dissolution of aragonite followed by precipitation of calcite, which would have accounted for the substantial increase in pore-water Sr^{2+} content, possibly leading to the formation of Celestine ($SrSO_4$) (Baker, 1986; Baker and Bloomer, 1988; Swart and Guzikowski, 1988; Swart and Burns, 1990; Swart et al., 1993), which was noticed between 163 and 393 mbsf (Betzler et al., 2017). The complete absence of pteropods and their fragments below 1.5 Myr owing to their present position above ALy, suggests diagenetic/post-deposition dissolution or significant shoaling of ACD.

5.2. Pteropod abundances/preservation in the equatorial Indian Ocean

The analyses of the last 24 Myr on IODP 359 Expedition Sites U1467 and U1468 have yielded the presence of fossil pteropods shells restricted only to the sediments of the last 1 Myr, whereas the presence of fragments was noted until 1.5 Myr. The variations in the pteropod abundance/preservation in the past 1 Myr record suggests systematic high and low-frequency variations in the aragonite content. Seawater chemistry had a primary impact on pteropod preservation. The study conducted by Betzler et al. (2017) using the sediments from Site U1467 shows a decrease in the SO_4^{2-} concentration and alkalinity in the interstitial fluid geochemistry indicate that significant remineralization of organic material has occurred below 50 mbsf. An odor of H_2S was also reported upon core recovery and squeezing of the whole-round samples, suggesting the bacterial sulfate reduction (BSR). Within the well-preserved record, a characteristic very low abundance to complete absence of pteropod shells was noted during MBDI. The long-term records of pteropod preservation from the equatorial Indian Ocean are very few and limited to past 600 kyr (Cullen and Droxler, 1990; Droxler et al., 1990). The present record for the last 1 Myr is compared with other records from the Indian Ocean, which shows regional similarity in pteropod abundance/preservation (Fig. 6). In ODP Hole 716A, pteropods occurred exclusively during the period between 450 and 150 kyr

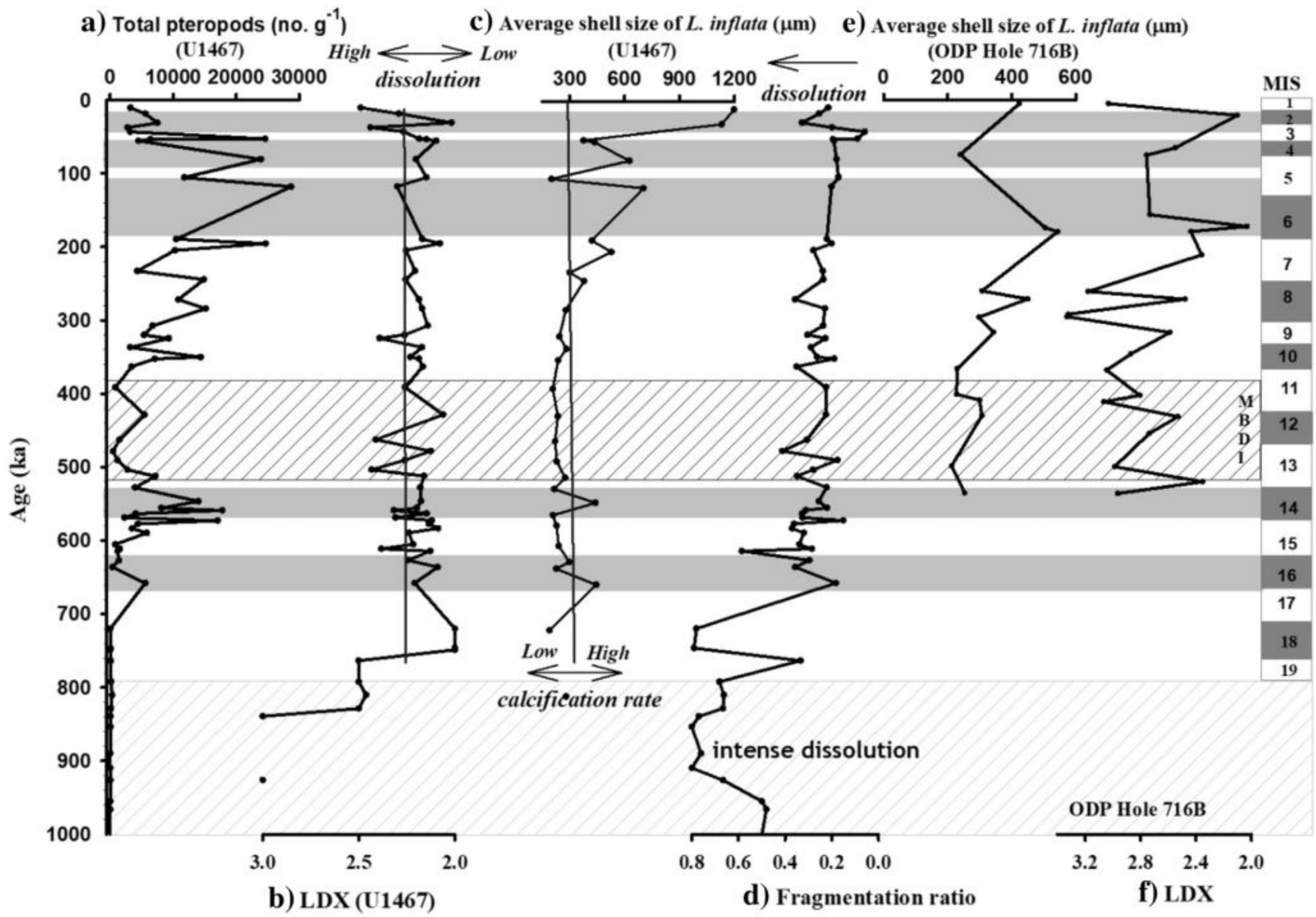

Fig. 5. Aragonite preservation and dissolution proxies (a) total pteropods (no. g^{-1}) (b) LDX (c) average shell size of *L. inflata* (μm) and (d) fragmentation ratio (fragments/fragments + total pteropods) for the past 1 Myr recorded in the core of Site U1467 as a function of time with MIS. The results are compared with the (e) LDX and average shell size of *L. inflata* from (f) ODP Hole 716B (Wall-Palmer et al., 2013). Shaded portions mark intense dissolution during MBDI. (The vertical solid line indicates the average value).

(Sarkar and Gupta, 2009). The characteristic global deglacial preservation spike was not seen in the Maldives record, but a smaller amplitude spike was noted during MIS 2. These global deglacial spikes occurred between 19 and 12 kyr in the Indian, the Pacific, and the Atlantic (see Sijinkumar et al., 2015 and references therein). It is centered at 13.5 ka BP in the Pacific, whereas in the Gulf of Mexico, high abundance/preservation of pteropod is encountered between 15 and 12.5 kyr. However, in the Equatorial Atlantic, it is centered between 13.5 and 14 kyr (Wiseman, 1965). The timing of the preservation spike in the Indian Ocean is consistent between 19 and 14 kyr, while the exact timing of the Andaman Sea preservation spike is between 19 and 15.5 kyr (Sijinkumar et al., 2015), while in the eastern Arabian Sea, the preservation spike off Goa is reported at 17.8–15 kyr (Singh et al., 2006). A preservation spike is observed between 18.8 and 14 kyr in the Gulf of Aden (Almogi-Labin et al., 2000) and between 17 and 13 kyr in the western Arabian Sea (Klöcker et al., 2006).

High abundances of pteropod species and total pteropods were seen during glacial periods and glacial to interglacial transitions. During interglacial to glacial transition stages, pteropods abundance/preservation was low. The most prominent period of best preservation of pteropods was centered at Eemian interglacial (MIS 5e) (Fig. 5) which is an exception when compared to other interglacial periods (MIS 7, 9, 11, 13), possibly the sea-level high stand favoring pteropod preservation by flooding the atoll and thereby producing high amounts of aragonite and mud, which were then exported and deposited in the inner sea (e.g. Siddall et al., 2003; Rohling et al., 2009). Similarly, pteropod minimum during early MIS 6 corresponds to the lowered sea level (Siddall et al., 2003; Rohling et al., 2009). Variations in the input are directly tied to alternate flooding and exposure of the shallow carbonate banks and, therefore, are a direct result of late Pleistocene climate-induced sea-level fluctuations Boardman et al., 1986; Droxler and Schlager, 1985; Reymer et al., 1985). They have described and summarized this concept as "carbonate high-stand shedding." In this case, therefore, high aragonite content in periplatform sediments should correspond to interglacial stages (the sea-level high stand), whereas low aragonite content should correspond to glacial intervals (sea-level low stand). But this is not seen in the pteropod records (except for MIS 5) with high abundances of the pteropods during glacial periods and low abundance/preservation during interglacial periods. Thus, according to the results obtained here, the good aragonite preservation during glacial periods can be attributed to very low atmospheric CO_2, enhanced ventilation and strengthened influx of Subantarctic Mode and Antarctic Intermediate Waters (SAMW-AAIW) and weakening of oxygen minimum zone (OMZ) (Böning and Bard, 2009).

The Indian Ocean pteropods belong ecologically to the epipelagic non-migratory group or the mesopelagic migratory species. The abundance of mesopelagic species *L. inflata* in the assemblage reflects increasing water depth; on the other hand, the predominance of *C. acicula, C. chierchiae,* and *C. virgula* suggests shallow water condition. The absolute abundances of mesopelagic and epipelagic species varied frequently during the last 1200 kyr (Fig. 4). Variations in the abundance of epipelagic over mesopelagic indicate fluctuation in the nature and

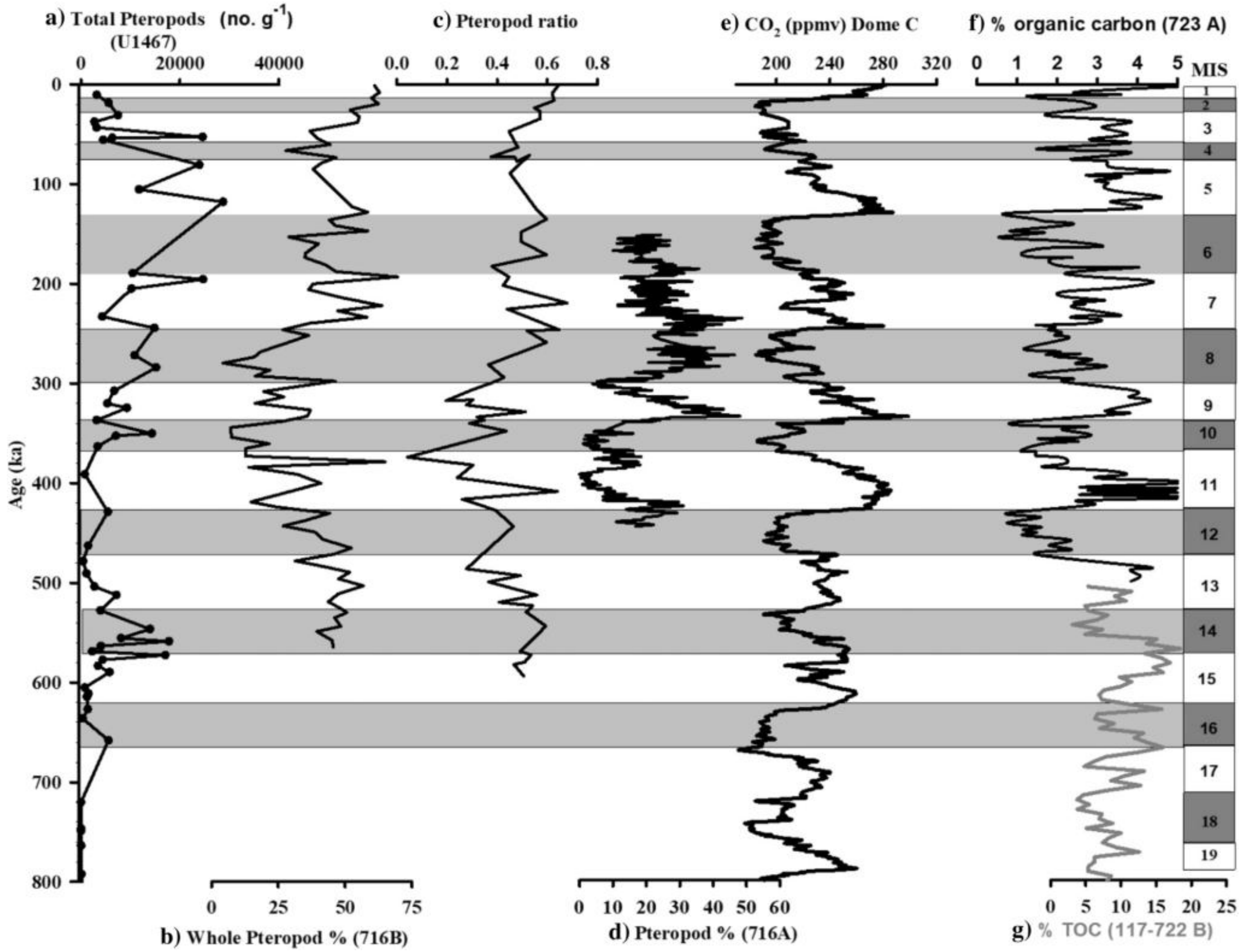

Fig. 6. A comprehensive record of the available Pleistocene pteropods abundances vs. atmospheric CO_2 and monsoon productivity proxies from the Indian Ocean with respect to MIS and age. (a) total pteropod abundance per gram in sediments from Site U1467, (b) pteropod% in ODP Hole 716B (Cullen and Droxler, 1990), (c) pteropod ratio in ODP Site 716B (Droxler et al., 1990), (d) pteropod (%) in ODP Hole 716A (Sarkar and Gupta, 2009), (e) atmospheric CO_2 (ppmv) from Dome C ice core (Lüthi et al., 2008), (f) percent of organic carbon from ODP Site 723A (Emeis et al., 1995) and (g) Total organic carbon (%) from Leg 117 Site 722B (Murray and Prell, 1991).

position of oxycline (Almogi-Labin et al., 1991, 1998) or changes in the water column stratification/ventilation. Variations in the relative abundance of epipelagic and mesopelagic pteropods were used to construct fluctuations in the nature of OMZ in the central Red Sea (Almogi-Labin et al., 1986, 1991), which is related to climatic fluctuations. Similarly, Rai et al. (2008) used pteropod abundance changes for reconstructing the strength of the OMZ in the northwestern Arabian Sea. Strong OMZ or highly oxygen-depleted water was common in the Western Indian Ocean during high surface-water productivity associated with monsoon upwelling (Schulte et al., 1999; Sarkar and Gupta, 2009). The dissolved-oxygen content decreases rapidly below 300 m depth and reaches a minimum between 600 and 1200 m depth (Sarkar and Gupta, 2009). A more intense and vertically more extended OMZ would favor the increase of epipelagic, mixed layer inhabitant pteropod in the fossil assemblage. During the past 1200 kyr, mesopelagic pteropods were dominant in the glacial stages while the epipelagic forms were mostly associated with interglacial stages which indicate stratification during warm periods and well-aerated intermediate water, related to cold climate. The significant periods of enhanced ventilation/mixing were seen during MIS 14 to 13 transitions, MIS 8, MIS 6 to 5 transition, MIS 3 and 2. These periods are also in phase with higher production of total pteropods, indicating good ventilation and excessive regeneration of intermediate-water circulation, which in turn weakened the OMZ and favored the pteropod preservation. The prominent stratification events are seen during 900 kyr to 600 kyr, MIS 9, late MIS 7, late MIS 5 and late MIS 2 to early Holocene, where abundances of epipelagic pteropods dominated over mesopelagic species, which suggests an intensification of the summer monsoon and results in high productivity, strong OMZ and intensified water column stratification. The high abundance of mesopelagic taxa during the glacial time in the Andaman Sea suggested the prevalence of significant ventilation of deep water due to enhanced deep winter mixing resulted by weaker OMZ and deepening of ACD (Sijinkumar et al., 2010). The high abundances of mesopelagic pteropods over epipelagic species along with better preservation during glacial periods suggest weakened summer monsoon.

5.3. *Mode of pteropod preservation, oceanic carbonate saturation, and climate-induced dissolution events*

Past variations in deep ocean chemistry were interpreted by studying in-life pteropod dissolution from sediments retrieved well

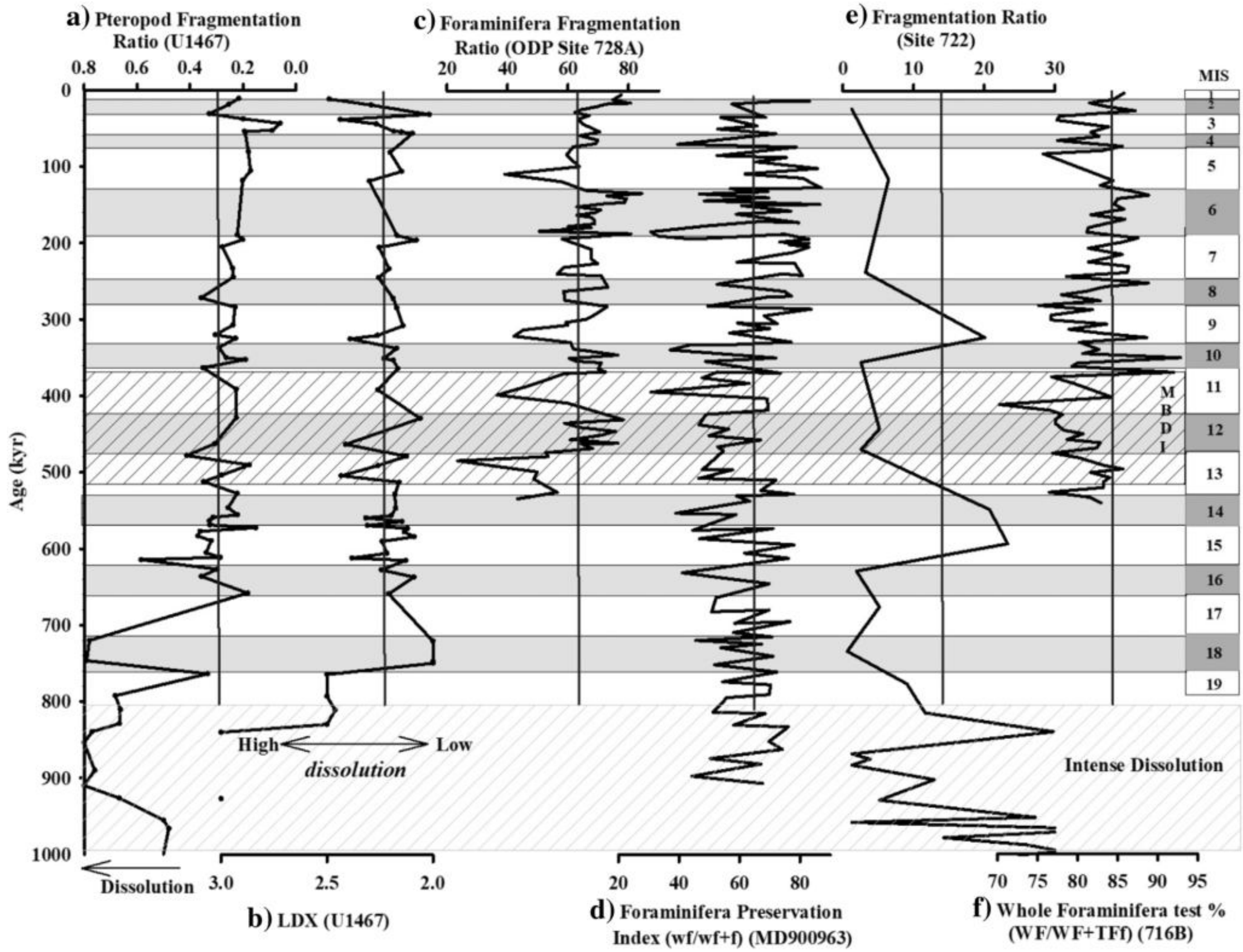

Fig. 7. Comparison of carbonate dissolution proxies from the present study with the available records of foraminifera fragmentation indices. (a) fragmentation ratio (Total fragments/Total fragments + total pteropods) recorded in the core of Site U1467, (b) LDX of Site U1467 (c) Foraminiferal fragmentation ration of ODP Site 728A (Rai and Das, 2011), (d) Foraminifera preservation index of the Core MD900963 (Bassinot et al., 1994), (e) FRAG (Foraminiferal Fragmentation Index) of Site 722 (Kawagata et al., 2006) and (f) foraminifera Fragmentation ratio of ODP Site 716B (Cullen and Droxler, 1990).

above the aragonite lysocline (Wall-Palmer et al., 2013). Whereas, post-depositional dissolution of the pteropod shells can be studied from sediments recovered close to or below aragonite lysocline. The core of Site U1467 was retrieved well above the present-day aragonite lysocline (Fig. 1) and provided a good opportunity to study both pteropod in-life dissolution and the changes in aragonite lysocline associated with changes in ocean chemistry. The increase in fragmentation, decrease in absolute abundance, and progressive modification of pteropod assemblages with depth is accompanied by a decrease in aragonite content. The complete wipeout of pteropods beyond 1.5 Myr involves all the species in the assemblage irrespective of any preferential dissolution due to the post-depositional changes as described in Section 5.1. Within the preserved record, the dissolution proxies, such as pteropods fragmentation ratio and average shell size of *L. inflata*, all point toward better preservation during the glacial stages (MIS 16, 14, 8, 6, 4, 3 and 2) with the exceptions to MIS 12 and 10 during MBDI. Previous studies have shown that reduced availability of calcium carbonate in water leads to reduced calcification rate, which can be deduced from the condensed linear extension of shells at apertural margin resulting in the production of small shells (Comeau et al., 2012; Wall-Palmer et al., 2013).

The published laboratory studies on pteropods also show reduced calcification rates and enhanced in-life shell dissolution with decreasing carbonate saturation (Orr et al., 2005; Fabry et al., 2008; Lischka et al., 2011; Comeau et al., 2012; Bednaršek et al., 2012). Examination of multiple dissolution proxies in this study has shown that in-life dissolution is the dominant process modifying the characteristics of size factor of sediments as indicated by the downcore variation in the size of *L. inflata*. The state of preservation of aragonitic pteropods at Site U1467 over the last 1 Myr ranging from good to moderate (i.e., Stage 2–3), moderate to poor (Stage 3–4) and very poor preservation (Stage > 4) at few time periods indicates climate-induced changes in oceanic carbonate saturation, fluctuations in aragonite compensation depth and global dissolution events (Almogi-Labin et al., 1986, 1991; Wall-Palmer et al., 2013).

Enhanced atmospheric CO_2 levels can lead to ocean acidification and the resultant reduced availability of carbonate ions are likely to make waters under-saturated with respect to aragonite affecting the pteropod calcification with weaker shells and damaged outer layers of aragonite (Bednaršek et al., 2012b; Comeau et al., 2012). Very few studies have presented the downcore abundance/preservation record of pteropod fossils from the Indian Ocean for a longer time scale (Cullen and Droxler, 1990; Droxler et al., 1990; Wall-Palmer et al., 2013). Hence the relationship between atmospheric CO_2 and pteropod preservation on a longer time scale is virtually unknown. The comparison with the recent study using *L. inflata* shell size and LDX has shown that the significant variations in in-life shell dissolution and calcification rate are driven by variations in the surface water carbonate concentration (Wall-Palmer et al., 2013). LDX is considered to be an efficient tool to understand the subtle changes in aragonite preservation (Gerhardt and Henrich, 2001; Klöcker et al., 2006), and this proxy is suitable for Site U1467 because of the occurrence of different types (transparent and opaque) of *L. inflata*. The state of preservation of pteropods, displaying distinct variation throughout the core length and the preservation records of the Indian Ocean are in good agreement with other records from the previous studies (Fig. 5). Wall-Palmer et al. (2013) have effectively used fossil pteropod proxies by comparing Vostok atmospheric CO_2 record as the proxies for surface ocean carbonate concentration, calcification rate, and surface ocean carbonate concentration. This was based on the assumption that the surface water dissolved CO_2 content is in equilibrium with atmospheric CO_2 concentrations, which directly affect the surface water carbonate saturation (Wall-Palmer et al., 2013). The average shell size of *L. inflata*, LDX, and fragmentation ratio in U1467 record show that the in-life dissolution of pteropods shell is more frequent during interglacial periods than glacial periods, which are the periods corresponding to low atmospheric CO_2 concentrations (Fig. 6). The average shell size of the *L. inflata* is higher during the periods of low atmospheric CO_2 concentrations and the resulting high surface water carbonate saturation, indicating very poor in-life dissolution. These findings corroborate with the results from the Caribbean Sea and the Maldives, Indian Ocean cores (Wall-Palmer et al., 2013). The glacial periods such as MIS 16, 14, 6, 4 and 2 are characterized by the presence of larger *L. inflata* shells and low LDX values suggesting better calcification in the aragonite-saturated water column. These glacial periods were coinciding with low CO_2 concentration in the atmosphere as well as very low monsoon productivity (Fig. 6). The good correlation of reduced atmospheric CO_2 concentration and larger average *L. inflata* shell size indicates that the in-life shell dissolution of *L. inflata* is directly related to atmospheric CO_2 levels (Wall-Palmer et al., 2013).

There are several late Quaternary records of carbonate preservation based on foraminifera dissolution proxies (Peterson and Prell, 1985a, 1985b; Cullen and Droxler, 1990; Murray and Prell, 1991, Bassinot et al., 1994; Kawagata et al., 2006; Rai and Das, 2011), whereas there are very limited number of records based on pteropods proxies (Fig. 7). The pteropod preservation records are complementing the findings of dissolution events reconstructed on the basis of foraminifera carbonate dissolution proxies. Besides these, pteropods proxies like LDX and the variation in the shell size of *L. inflata* provide precise information on past oceanic carbonate saturation. Pteropods dissolution proxies such as pteropods fragmentation ratio and average shell size of *L. inflata* show better preservation during glacial stages (MIS 16, 14, 8, 6, 4, 3 and 2 and dissolution event during MIS 11, 12, and 13 (MBDI) which is showing good correlation with foraminifera dissolution proxies (Fig. 7). Typically, smaller shells, higher LDX values (2.5 to 3) and high fragmentation ratio occurred from 520 kyr to 380 kyr (MIS 13 to 11) are coinciding with MBDI. Similar long intervals of poor pteropod preservation also observed in deeper water cores from Ninety-east Ridge (Peterson and Prell, 1985b), Maldives (Droxler et al., 1983, 1990; Cullen and Droxler, 1990) and the carbonate preservation pattern appear to be offset from the $\delta^{18}O$ glacial/interglacial records. Preservation maxima occur at glacial-to-interglacial transitions, whereas dissolution maxima occur at interglacial-to-glacial transitions (Figs. 5 and 7). This particular pattern has been suggested to be global in several studies (e.g., Crowley, 1983, [CSL STYLE ERROR: reference with no printed form.], [CSL STYLE ERROR: reference with no printed form.]). The data set of Peterson and Prell (1985a, 1985b) also shows evidence of the existence of a longer cycle of poor carbonate preservation during the MBDI between 300 and 600 kyr. This supercycle is also well developed in the carbonate records of the equatorial Pacific Ocean, where a poor carbonate interval occurred between 200 and 500 kyr (Hays et al., 1969; Adelseck and Anderson, 1978; Moore Jr et al., 1982; Vincent and Berger, 1985; Farrell and Prell, 1987, 1989), North Atlantic Ocean, where aragonite lows clearly define the 200 to 450 kyr interval (Crowley, 1985), periplatform sites of the Maldives and the Bahamas, as well as by an increase in pteropod fragmentation in the shallow sites (500–700 m). This trend is even more evident in the Bahamas where the aragonite disappeared during the late Pliocene. But the aragonite values reached very high during the early Pliocene and late Pleistocene. MBDI represents a major perturbation to the global ocean carbon system (see Barker et al., 2006) and resulted in under-saturation of carbonate in seawater. It is considered as a prominent carbonate dissolution episode. Flores et al. (2003) noted the correspondence between high $CaCO_3$ and the increased abundance of coccolith *Gephyrocapsa*, contemporaneous with enhanced dissolution during the Mid-Brunhes in ODP Site 1089. Significant changes in the coccolithophore assemblages and reduced diversity were also reported from the Central Indian Ocean Basin during MBDI (Nath et al., 2013). All pteropod abundance drops to extremely low numbers during MBDI. Late MIS 5 (112 to 98 kyr) has also shown intense in-life carbonate dissolution marked by smaller *L. inflata* shells and high LDX stages. The co-occurrence of carbonate dissolution events in the Red Sea and the Indian Ocean, with no direct deep-water connection between the two basins, make changes in deep water circulation as the primary cause of these widespread deep-water dissolution events unlikely (Bassinot et al., 1994; Almogi-Labin et al., 1998).

Other possible factor controlling pteropod preservation may be the productivity changes, due to change in monsoon intensity in this region (See Singh and Rajarama, 1997; Singh, 1998). High abundance and good preservation of pteropods during the glacials are associated with lower abundance of *Globigerinabulloides*, suggesting that pteropod preservation is strongly influenced by the strength of summer monsoon in the Indian Ocean (Sijinkumar et al., 2010). Upwelling and resulting high productivity greatly affect the accumulation of aragonite in sediments, particularly pteropod shells, owing to their vulnerability to dissolution. High preservation probably represents a period of low productivity and well mixed intermediate-water. The low organic carbon values were seen during glacial periods, which correlated with better preservation of pteropods (Fig. 6). Monsoon-induced productivity changes can lead to strong OMZ (Von Rad et al., 1999). Aragonite preservation seems to be also controlled by the intensity of the OMZ, being extremely weak during glacial periods of the reduced summer monsoon. In the Indian Ocean, OMZ depth is demarcated between 150 and 1200 m (Reichart et al., 2002; Sarkar and Gupta, 2009). The core locations being collected within the OMZ depth, the surface and deep-water conditions at Site U1467 were coupled during Pleistocene, which suggests pteropod populations were influenced by in situ changes in food availability and oxygen levels. The upwelling regions which are characterized by high biological productivity affect the preservation of sedimentary carbonates, particularly pteropods owing to their vulnerability to dissolution. Globally upwelling regions are characterized by poor pteropod preservation (Berger, 1978; Ganssen and Lutze, 1982; Gerhardt and Henrich, 2001), which is attributed to the high concentration of dissolved inorganic carbon (DIC), resulting from high input and demineralization of organic matter, lowering the pH (Millero et al., 1998). Supralysoclinal or biologically mediated carbonate dissolution through the decomposition of organic matter within the sediments lowers pore-water pH (Milliman et al., 1999). The good correlation of poor preservation of pteropods with organic carbon record (Fig. 6) and high abundances of epipelagic species over mesopelagic (Fig. 4) suggests significantly stronger monsoon during 900 kyr to 600 kyr, MIS 9, MIS 7, late MIS 5 and late MIS 2 to early Holocene.

6. Conclusions

IODP Site U1467 (together with U1468) provides a long carbonate preservation record from the Indian Ocean which witnessed pteropod abundance/preservation over the past 1.2 Myr, which is consistent with the presence of aragonite content in sediments. The aragonite content generally correlates well with total pteropod abundance estimated. However, the aragonite is re-precipitated as calcite at depth, at the expense of pteropod dissolution, which is apparent from increasing Sr^{2+} ion in the pore-water. Relatively, a high abundance of mesopelagic pteropods over epipelagic forms during certain periods can be explained by the well-aerated intermediate mixed layer with weak OMZ. The mesopelagic to epipelagic pteropod ratio also shows periods of enhanced ventilation/mixing during MIS 14 to 13 transition, MIS 8, MIS 6 to 5 transition, MIS 3 and 2. The prominent water column stratification events due to the intensification of summer monsoon are seen during 900 kyr to 600 kyr, MIS 9, MIS 7, late MIS 5 and late MIS 2 to early Holocene where abundances of epipelagic pteropods dominated over mesopelagic species.

The Mid-Brunhes Dissolution Interval (MBDI) is characterized by poor aragonite preservation clearly defined by the lower preservation of pteropod shells during MIS 11 and 13 and then increases further downcore. The proxies for in-life pteropod shell dissolution indicate a significant calcification in the glacial periods (MIS 16, 14, 6, 4 and 2) and there is no sign of dissolution under aragonite-saturated water column. The glacial periods mark the reduced atmospheric CO_2concentration and low monsoon productivity. The good correlation of reduced atmospheric CO_2 concentration and larger average *L. inflata* shell size indicates that the in-life shell dissolution of *L. inflata* is directly related to atmospheric CO_2 levels, which corroborate the earlier findings from the Indian Ocean (ODP 115 Hole 716B) and the Caribbean sites. However, these results demonstrate that the ability to calcify and maintain shells of late Pleistocene pteropods were severely affected by the surface water carbonate chemistry and these findings are significant in the present scenario of increased dissolution of aragonite pteropod shells owing to the anthropogenic input of CO_2.

Acknowledgments

This research is based on the samples provided by the International Ocean Discovery Program (IODP). The authors acknowledge the dedicated effort of the drilling crew, ship's crew, and scientific staff of the Drill ship JOIDES Resolution and the scientific participants. Participation of BN in Expedition 359 was supported by IODP India at NCPOR, Goa. Post-cruise onshore lab facilities were provided by Director, CSIR-National Institute of Oceanography and part expenses were met from CSIR XII Plan Network Project GEOSINKS. Mr. Sarunlal and Ms. Tanvi Mungekar helped in preparing the samples. We thank the three anonymous reviewers for their constructive comments, which helped us to improve the manuscript. SE acknowledges DST-INSPIRE Junior Research Fellowship (IF170505) funded by the Department of Science and Technology, Government of India. AVS acknowledges the UGC, New Delhi for the BSR Research Start-Up-Grant (No. F.30-366/2017) and SERB, New Delhi for the ECR Grant (ECR/2017/000818).

Appendix A. Supplementary data

Supplementary data to this article can be found online at https://doi.org/10.1016/j.palaeo.2019.109313.

References

Adelseck, C.G., Anderson, T.F., 1978. The late Pleistocene record of productivity fluctuations in the eastern equatorial Pacific Ocean. Geology 6, 388–391.

Almogi-Labin, A., 1982. Stratigraphic and Paleoceanographic significance of late Quaternary pteropods from deep-sea cores in the Gulf of Aqaba (Elat) and northern most Red Sea. Marine Micropaleontology 7, 53–72.

Almogi-Labin, A., Luz, B., Duplessy, J.C., 1986. Quaternary paleo-oceanography, pteropod preservation and stable isotope record of the Red Sea. Palaeogeogr. Palaeoclimatol. Palaeoecol. 57, 195–211.

Almogi-Labin, A., Hemleben, C., Meischner, D., Erlenkeuser, H., 1991. Paleoenvironmental events during the last 13,000 years in the central Red Sea as recorded by pteropoda. Paleoceanography 6, 83–98.

Almogi-Labin, A., Hemleben, C., Meischner, D., 1998. Carbonate preservation and climatic changes in the central Red Sea during the last 380 kyr as recorded by pteropods. Mar. Micropaleontol. 33, 87–107.

Almogi-Labin, A., Schmiedl, G., Hemleben, C., Siman-Tov, R., Segl, M., Meischner, D., 2000. The influence of the NE winter monsoon on productivity changes in the Gulf of Aden, NW Arabian Sea, during the last 530 ka as recorded by foraminifera. Mar. Micropaleontol. 40, 295–319.

Aubert, O., Droxler, A., 1996. Seismic stratigraphy and depositional signatures of the Maldives carbonate system (Indian Ocean). Mar. Pet. Geol. 13 (5), 503–536.

Baker, P.A., 1986. Pore-water chemistry of carbonate-rich sediments, Lord Howe Rise, southwest Pacific-Ocean. Initial reports of the deep-sea drilling project 90, 1249–1256.

Baker, P.A., Bloomer, S.H., 1988. The origin of celestite in deep-sea carbonate sediments. Geochim. Cosmochim. Acta 52, 335–339.

Barker, S., Archer, D., Booth, L., Elderfield, H., Henderiks, J., Rickaby, R.E.M., 2006. Globally increased pelagic carbonate production during the Mid-Brunhes dissolution interval and the CO_2 paradox of MIS 11. Quat. Sci. Rev. 25, 3278–3293.

Bassinot, F.C., Beaufort, L., Vincent, E., Labeyrie, L.D., Rostek, F., Müller, P.J., Quidelleur, X., Lancelot, Y., 1994. Coarse fraction fluctuations in pelagic carbonate sediments from the tropical Indian Ocean: a 1500-kyr record of carbonate dissolution. Paleoceanography and Paleoclimatology 9, 579–600.

Bé, A.W.H., Gilmer, R.W., 1977. A zoogeographic and taxonomic review of Euthecosomatous Pteropoda. Oceanic micropaleontology 1 (6), 733–808.

Bednaršek, N., Tarling, G.A., Bakker, D.C.E., Fielding, S., Cohen, A., Kuzirian, A., McCorkles, D., Lézé, B., Montagna, R., 2012. Description and quantification of pteropod shell dissolution: a sensitive bioindicator of ocean acidification. Glob. Chang. Biol. 18 (7), 2378–2388.

Bednaršek, N., Tarling, G.A., Bakker, D.C.E., Fielding, S., Jones, E.M., Venables, H.J., Ward, P., Kuzirian, A., Lézé, B., Feely, R.A., Murphy, E.J., 2012b. Extensive dissolution of live pteropods in the Southern Ocean. Nat. Geosci. 5 (12), 881.

Berger, W.H., 1978. Deep-sea carbonate: pteropod distribution and the aragonite compensation depth. Deep-Sea Res. 25, 447–452.

Betzler, C., Hübscher, C., Lindhorst, S., Reijmer, J.J.G., Römer, M., Droxler, A., Fürstenau, J., Lüdmann, T., 2009. Monsoon-induced partial carbonate platform drowning (Maldives, Indian Ocean). Geology 37 (10), 867–870.

Betzler, C., Fürstenau, J., Lüdmann, T., Hübscher, C., Lindhorst, S., Paul, A., Reijmer, J.J.G., Droxler, A.W., 2013a. Sea-level and ocean-current control on carbonate-platform growth, Maldives, Indian Ocean. Basin Res. 25 (2), 172–196.

Betzler, C., Lüdmann, T., Hübscher, C., Fürstenau, J., 2013b. Current and sea-level signals in periplatform ooze (Neogene, Maldives, Indian Ocean). Sediment. Geol. 290, 126–137.

Betzler, C., Eberli, G.P., Kroon, D., Wright, J.D., Swart, P.K., Nath, B.N., Alvarez-Zarikian, C.A., Alonso-García, M., Bialik, O.M., Blättler, C.L., Guo, J.A., Haffen, S., Horozal, S., Inoue, M., Jovane, L., Lanci, L., Laya, J.C., Mee, A.L.H., Lüdmann, T., Nakakuni, M., Niino, K., Petruny, L.M., Pratiwi, S.D., Reijmer, J.J.G., Reolid, J., Slagle, A.L., Sloss, C.R., Su, X., Yao, Z., Young, J.R., 2016. The abrupt onset of the modern South Asian Monsoon winds. Sci. Rep. 6, 29838.

Betzler, C., Eberli, G.P., Alvarez Zarikian, C.A., the Expedition 359 Scientists, 2017. Maldives monsoon and sea-level. In: Proceedings of the International Ocean Discovery Program, 359. Station, TX (International Ocean Discovery Program), College. https://doi.org/10.14379/iodp.proc.359.2017.

Betzler, C., Eberli, G.P., Lüdmann, T., Reolid, J., Kroon, D., Reijmer, J.J.G., Swart, P.K., Wright, J., Young, J.R., Alvarez-Zarikian, C., Alonso-García, M., 2018. Refinement of Miocene sea level and monsoon events from the sedimentary archive of the Maldives (Indian Ocean). Progress in Earth and Planetary Science 5 (1), 5.

Boardman, M.R., Neumann, A.C, Baker, P.A., Dulin, L.A., Kenter, R.J., Hunter, G.E., Kiefer, K.B., 1986. Banktop responses to Quaternary fluctuations in sea-level recorded in periplatform sediments. Geology 14 (1), 28–31.

Böning, P., Bard, E., 2009. Millennial/centennial-scale thermocline ventilation changes in the Indian Ocean as reflected by aragonite preservation and geochemical variations in Arabian Sea sediments. Geochim. Cosmochim. Acta 73, 6771–6788.

Comeau, S., Alliouane, S., Gattuso, J.P., 2012. Effects of ocean acidification on overwintering juvenile Arctic pteropods *Limacina helicina*. Mar. Ecol. Prog. Ser. 456, 279–284.

Crowley, T.J., 1983a. Calcium-carbonate preservation patterns in the central North Atlantic during the last 150,000 years. Marine Geology51, 1–14.

Crowley, T.J., 1985. Late Quaternary carbonate changes in the North Atlantic and Atlantic/Pacific comparisons. In Sundquist, E. T, and Broecker, W. S. (Eds.), The Carbon Cycle and Atmospheric CO_2: Natural Variations, Archean to Present: Geophysical Monograph vol. 32, 271–284.

Crowley, T.J., 1983b. Depth-dependent carbonate dissolution changes in the eastern North Atlantic during the last 170,000 years. Mar. Geol. 54, 25–31.

Cullen, J.L., Droxler, A.W., 1990. Late Quaternary variations in planktonic foraminifer faunas and pteropod preservation in the equatorial Indian Ocean. Proc. Ocean Drill. Program Sci. Results 115, 579–588.

Droxler, A.W., Schlager, W., 1985. Glacial/interglacial sedimentation rates and turbidite frequency in the Bahamas: a clear case of carbonate shedding during high sea-level stands. Geological Society Amsterdam, Abstract Programs; United States. Geology 13, 799–802.

Droxler, A.W., Schlager, W., Whallon, C.C., 1983. Quaternary aragonite cycles and oxygen isotope record in Bahamian carbonate ooze. Geology 11 (4), 235–239.

Droxler, A.W., Haddad, G.A., Mucciarone, D.A., Cullen, J.L., 1990. Pliocene-Pleistocene aragonite cyclic variations in Holes 714A and 716B (the Maldives) compared with Hole 633A (the Bahamas): records of climate-induced $CaCO_3$ preservation at intermediate water depths. Proc. Ocean Drill. Program Sci. Results 115, 539–577.

Emeis, K.C., Anderson, D.M., Doose, H., Kroon, D., Schulz-Bull, D., 1995. Sea-surface temperatures and the history of monsoon upwelling in the northwest Arabian Sea during the last 500,000 years. Quat. Res. 43, 355–361.

Emery, W.J., 2001. Water types and water-masses. Encyclopedia of Ocean Sciences 6,

3179–3187.
Fabry, V.J., Seibel, B.A., Feely, R.A., Orr, J.C., 2008. Impacts of ocean acidification on fauna and ecosystem processes. ICES J. Mar. Sci. 65, 414–432.
Farrell, J.W., Prell, W.L., 1987. Climate forcing of calcium carbonate sedimentation: a 4.0 my record from the central Equatorial Pacific. EOS, Transactions, American Geophysical Union 68, 333.
Farrell, J.W., Prell, W.L., 1989. Climatic change and CaCO3 preservation: an 800,000 year bathymetric reconstruction from the central equatorial Pacific Ocean. Paleoceanography 4, 447–466.
Flores, J.A., Marino, M., Sierro, F.J., Hodell, D.A., Charles, C.D., 2003. Calcareous plankton dissolution pattern and coccolithophore assemblages during the last 600 kyr at ODP Site 1089 (Cape Basin, South Atlantic): paleoceanographic implications. Paleogeography, Paleoclimatology, Paleoecology 196, 409–426.
Ganssen, G., Lutze, G.F., 1982. The aragonite compensation depth at the northeastern Atlantic continental margin. Meteor'Forsch.-Ergebnisse 36, 57–59.
Gardner, J.V., 1975. Late Pleistocene carbonate dissolution cycles in the eastern equatorial Atlantic. In: Sliter, W.V., Be, A.W.H., Berger, W.H. (Eds.), Dissolution of Deep-Sea Carbonates. Special Publication, Cushman Foundation for Foraminiferal Research 13. pp. 129–141.
Gerhardt, S., Henrich, R., 2001. Shell preservation of *Limacina inflata* (Pteropoda) in surface sediments from the Central and South Atlantic Ocean: a new proxy to determine the aragonite saturation state of water-masses. Deep-Sea Res. I Oceanogr. Res. Pap. 48 (9), 2051–2071.
Gerhardt, S., Groth, H., Rühlemann, C., Henrich, R., 2000. Aragonite preservation in late Quaternary sediment cores on the Brazilian Continental Slope: implications for intermediate water circulation. Int. J. Earth Sci. 88, 607–618.
Hays, J.D., Saito, T., Opdyke, N.D., Burckle, L.H., 1969. Pliocene-Pleistocene sediments of the equatorial Pacific: their paleo-magnetic biostratigraphic and climatic record. Geological Society America Bulletin 80 (8), 1481–1514.
Herman, Y., 1968. Evidence of climatic changes in Red Sea cores: means of correlations of quaternary successions. Congress of International Association for Quaternary Research, Salt Lake City 8, 325–348.
Howard, W.R., Prell, W.L., 1994. Late Quaternary $CaCO_3$ production and preservation in the Southern Ocean: implications for oceanic and atmospheric carbon cycling. Paleoceanography and Paleoclimatology 9 (3), 453–482.
Ivanova, E.V., 1985. Late Quaternary biostratigraphy and paleotemperatures of the Red Sea and the Gulf of Aden based on planktonic foraminifera and pteropods. Mar. Micropaleontol. 9 (4), 335–364.
Kalberer, M., Fischer, G., Pätzold, J., Donner, B., Segl, M., Wefer, G., 1993. Seasonal sedimentation and stable isotope records of pteropods off Cap Blanc. Mar. Geol. 113 (3–4), 305–320.
Kawagata, S., Hayward, B.W., Gupta, A.K., 2006. Benthic foraminiferal extinctions linked to late Pliocene–Pleistocene deep-sea circulation changes in the northern Indian Ocean (ODP Sites 722 and 758). Mar. Micropaleontol. 58 (3), 219–242.
Klöcker, R., Ganssen, G., Jung, S.J.A., Kroon, D., Henrich, R., 2006. Late Quaternary millennial scale variability in pelagic aragonite preservation off Somalia. Mar. Micropaleontol. 59 (3–4), 171–183.
Lischka, S., Büdenbender, J., Boxhammer, T., Riebesell, U., 2011. Impact of ocean acidification and elevated temperatures on early juveniles of the polar shelled pteropod*Limacinahelicina*: mortality, shell degradation, and shell growth. Biogeosciences 8, 919–932.
Lüdmann, T., Kalvelage, C., Betzler, C., Fürstenau, J., Hübscher, C., 2013. The Maldives, a giant isolated carbonate platform dominated by bottom currents. Mar. Pet. Geol. 43, 326–340.
Lüthi, D., Le Floch, M., Bereiter, B., Blunier, T., Barnola, J.M., Siegenthaler, U., Raynaud, D., Jouzel, J., Fischer, H., Kawamura, K., Stocker, T.F., 2008. High-resolution carbon dioxide concentration record 650,000-800,000 years before present. Nature 453, 379–382.
Malone, M.J., Baker, P.A., Burns, S.J., Swart, P.K., 1990. Geochemistry of periplatform carbonate sediments, Leg 115, Site 716 (Maldives Archipelago, Indian Ocean). In Proceedings of the Ocean Drilling Program, Scientific Results 115, 647–659.
Millero, F.J., Yao, W., Lee, K., Zhang, J.Z., Campbell, D.M., 1998. Carbonate system in the waters near the Galapagos Islands. Deep-Sea Res. II Top. Stud. Oceanogr. 45, 1115–1134.
Milliman, J.D., Troy, P.J., Balch, W.M., Adams, A.K., Li, Y.H., Mackenzie, F.T., 1999. Biologically mediated dissolution of calcium carbonate above the chemical lysocline? Deep-Sea Res. I Oceanogr. Res. Pap. 46, 1653–1669.
Moore Jr., T.C., Pisias, N.G., Dunn, D.A., 1982. Carbonate time series of the Quaternary and late Miocene sediments in the Pacific Ocean: a spectral comparison. Mar. Geol. 46, 217–233.
Murray, D.W., Prell, W.L., 1991. Pliocene to Pleistocene variations in calcium carbonate, organic carbon, and opal on the Owen Ridge, Northern Arabian Sea. Proc. Ocean Drill. Program Sci. Results 117, 343–355.
Nath, B.N., Sijinkumar, A.V., Borole, D.V., Gupta, S.M., Mergulhao, L.P., Mascarenhas-Pereira, M.B., Ramaswamy, V., Guptha, M.V., Possnert, G., Aldahan, A., Khadge, N.H., 2013. Record of carbonate preservation and the Mid-Brunhes climatic shift from a seamount top with low sedimentation rates in the Central Indian Basin. Boreas 42, 762–778.
Orr, J.C., Fabry, V.J., Aumont, O., Bopp, L., Doney, S.C., Feely, R.A., Gnanadesikan, A., Gruber, N., Ishida, A., Joos, F., Key, R.M., Lindsay, K., Maier-Reimer, E., Matear, R., Monfray, P., Mouchet, A., Najjar, R.G., Plattner, G., Rodgers, K.B., Sabine, C.L., Sarmiento, J.L., Schlitzer, R., Slater, R.D., Totterdell, I.J., Weirig, M., Yamanaka, Y., Yool, A., 2005. Anthropogenic Ocean acidification over the twenty-first century and its impact on calcifying organisms. Nature 437, 681–686.
Paul, A., Reijmer, J.J., Fürstenau, J., Kinkel, H., Betzler, C., 2011. Relationship between Late Pleistocene sea-level variations, carbonate platform morphology and aragonite production (Maldives, Indian Ocean). Sedimentology 59, 1640–1658.
Peterson, L.C., Prell, W.L., 1985a. Carbonate dissolution in recent sediments of the eastern equatorial, Indian Ocean: preservation and carbonate loss above the lysocline. Mar. Geol. 64 (3–4), 259–290.
Peterson, L.C., Prell, W.L., 1985b. Carbonate preservation and rates of climatic change: an 800 kyr record from the Indian Ocean. The carbon cycle and atmospheric CO_2: Natural variations Archean to present. Geophysical Monograph Series 32, 251–269.
Rai, A.K., Das, S.S., 2011. Late Quaternary changes in surface productivity and oxygen minimum zone (OMZ) in the northwestern Arabian Sea: micropaleontologic and sedimentary record at ODP site 728A. Journal of earth system science 120 (1), 113–121.
Rai, A.K., Singh, V.B., Maurya, A.S., Shukla, S., 2008. Ventilation of northwestern Arabian Sea Oxygen Minimum Zone during last 175 kyrs: a pteropod record at ODP Site 728A. Curr. Sci. 94, 480–485.
Reichart, G.J., Nortier, J., Versteegh, G.J.M., Zachariasse, W.J., 2002. Periodical breakdown of the Arabian Sea oxygen minimum zone caused by deep convective mixing. In: Clift, P.D., Kroon, D., Craig, J., Gaedicke, C. (Eds.), the Tectonic and Climatic Evolution of the Arabian Sea Region. Geol. Soc. Spec. Publ. 195 (1), 407–419.
Reid, P.C., Fischer, A.C., Lewis-Brown, E., Meredith, M.P., Sparrow, M., Andersson, A.J., Antia, A., Bates, N.R., Bathmann, U., Beaugrand, G., Brix, H., Dye, H., Edwards, M., Furevik, T., Gangstø, R., Ha'tu'n, H., Hopcroft, R.R., Kendall, M., Katsen, S., Keeling, R., Que're´, C.L., Mackenzie, F.T., Malin, G., Mauritzen, C., Jo'nO'lafsson, Paull, C., Rignot, E., Shimada, K., Vogt, M., Wallace, C., Wang, Z., Washington, R., 2009. Impacts of the oceans on climate change. Adv. Mar. Biol. 56, 1–150.
Reymer, J.J., Schlager, W., Droxler, A.W., 1985. SITE 632: Pliocene-Pleistocene sedimentation cycles in a Bahamian Basin. In Proceedings of the Ocean Drilling Program: Scientific results 101, 213.
Rohling, E.J., Grant, K., Bolshaw, M., Roberts, A.P., Siddall, M., Hemleben, C., Kucera, M., 2009. Antarctic temperature and global sea-level closely coupled over the past five glacial cycles. Nat. Geosci. 2 (7), 500–504.
Sabine, C.L., Key, R.M., Feely, R.A., Greeley, D., 2002. Inorganic carbon in the Indian Ocean: distribution and dissolution processes. Glob. Biogeochem. Cycles 16, 1067. https://doi.org/10.1029/2002GB001869.
Sarkar, S., Gupta, A.K., 2009. Deep-sea palaeoceanography of the Maldives Islands (ODP Hole 716A), equatorial Indian Ocean during MIS 12-6. J. Biosci. 34, 749. https://doi.org/10.1007/s12038-009-0066-7.
Sarma, V.V.S.S., Ono, T., Saino, T., 2002. Increase of total alkalinity due to shoaling of aragonite saturation horizon in the Pacific and Indian Oceans: influence of anthropogenic carbon inputs. Geophysical Research Letters 29 (20), https://doi.org/10.1029/2002GL015135.
Schott, F.A., Xie, S.P., McCreary, J.P., 2009. Indian Ocean circulation and climate variability. Rev. Geophys. 47. https://doi.org/10.1029/2007/rg000245.
Schulte, S., Rostek, F., Bard, E., Rullkötter, J., Marchal, O., 1999. Variations of oxygen-minimum and primary productivity recorded in sediments of the Arabian Sea. Earth Planetary Science Letters 173, 205–221.
Siddall, M., Rohling, E.J., Almogi-Labin, A., Hemleben, C., Meischner, D., Schmelzer, I., Smeed, D.A., 2003. Sea-level fluctuations during the last glacial cycle. Nature 423, 853–858.
Sijinkumar, A.V., Nath, B.N., Guptha, M.V.S., 2010. Late Quaternary record of pteropod preservation from the Andaman Sea. Mar. Geol. 275, 221–229.
Sijinkumar, A.V., Nath, B.N., Guptha, M.V., Ahmad, S.M., Rao, B.R., 2015. Timing and preservation mechanism of deglacialpteropod spike from the Andaman Sea, northeastern Indian Ocean. Boreas 44, 432–444.
Singh, A.D., 1998. Late Quaternary oceanographic changes in the eastern Arabian Sea: evidence from planktic foraminifera and pteropods. J. Geol. Soc. India 52, 203–212.
Singh, A.D., Rajarama, K.N., 1997. Distribution of pteropods in surface sediments from the continental shelf off North Kerala. J. Geol. Soc. India 49, 81–84.
Singh, A.D., Kroon, D., Ganeshram, R.S., 2006. Millennial-scale variations in productivity and OMZ intensity in the eastern Arabian Sea. Journal of Geological society of India 68, 369–377.
Swart, P.K., Burns, S.J., 1990. Pore-water chemistry and carbonate diagenesis in sediments from Leg 115: Indian Ocean. In Duncan, R.A., Backman, J., Peterson, L.C., et al. Proc. Ocean Drill. Program Sci. Results 115, 629–645.
Swart, P.K., Guzikowski, M., 1988. Interstitial-water chemistry and diagenesis of periplatform sediments from the Bahamas, ODP Leg 101. In Austin, J.A., Jr., Schlager, W., et al. Proc. Ocean Drill. Program Sci. Results 101, 363–380.
Swart, P.K., Isern, A., Elderfield, H., McKenzie, J.A., 1993. A summary of interstitial-water geochemistry of Leg 133. In McKenzie, J.a., Davies, P.J., Palmer-Julson, a., et al. Proceedings of Ocean Drilling Program, Scientific Result 133, 705–721.
Swart, P.K., Mackenzie, G.J., Eberli, G.P., Lüdmann, T., Betzler, C., 2019. Do drifts deposited adjacent to carbonate platforms record the signal of global carbon isotopic values? Sedimentology 66 (4), 1410–1426. https://doi.org/10.1111/sed.12580.
Tomczak, M., Godfrey, J.S., 2003. Regional Oceanography: an Introduction. Pergamon (Oxford) 229–252.
Van der Spoel, S., 1967. Euthecosomata, a Group with Remarkable Developmental Stages (Gastropoda, Pteropoda). J. Noorduijnen Zoon N.V, Gorinchem, Netherlands, pp. 375.
Vincent, E., Berger, W.H., 1985. Carbon dioxide and polar cooling in the Miocene: the Monterey hypothesis. The carbon cycle and atmospheric CO_2: Natural variations Archean to present 32, 455-468.
Von Rad, U., Schaaf, M., Michels, K.H., Schulz, H., Berger, W.H., Sirocko, F., 1999. A 5000-yr record of climate change in varved sediments from the oxygen minimum zone off Pakistan, Northeastern Arabian Sea. Quat. Res. 51 (1), 39–53.
Wall-Palmer, D., Smart, C.W., Hart, M.B., 2013. In-life pteropod shell dissolution as an indicator of past ocean carbonate saturation. Quat. Sci. Rev. 81, 29–34.
Wiseman, J.D.H., 1965. The changing rate of calcium carbonate sedimentation on the Equatorial Atlantic floor and its relation to continental Late Quaternary sediment cores from the North Atlantic Ocean. Reports of the Swedish Deep-Sea Expedition 7, 288–354.